



Article

Substrate Influences Temperature Sensitivity of Dissolved Organic Carbon (DOC) and Nitrogen (DON) Mineralization in Arid Agricultural Soils

Abdulaziz A. AlMulla ^{1,2}, Davey Jones ² and Paula Roberts ^{2,*}

¹ Department of Environmental Health, College of Public Health, Imam Abdulrahman Bin Faisal University, P.O. Box 1982, Dammam 31441, Saudi Arabia; aaalmulla@iau.edu.sa

² School of Environment, Natural Resources and Geography, Bangor University, Bangor, Gwynedd LL57 2UW, UK; d.jones@bangor.ac.uk

* Correspondence: p.roberts@bangor.ac.uk; Tel.: +44-1248-382976 (ext. 354997)

Received: 5 February 2018; Accepted: 27 April 2018; Published: 1 May 2018



Abstract: The bioavailability of nitrogen (N) in soil relies on the progressive breakdown of necromass protein to peptide and amino acid components and conversion to inorganic N forms. We understand the fluxes and pathways of the N cycle downstream from amino acids, but our understanding of the factors controlling peptide and amino acid mineralization, particularly in arid soils, is lacking. We investigated the influence of temperature on the rate of dissolved organic carbon (DOC) and nitrogen (DON) cycling in three agricultural soils from Saudi Arabia. Although the physical and chemical properties of the soils differed markedly, phospholipid fatty acid (PLFA) analysis revealed they had similar topsoil and subsoil microbial communities. Soils behaved similarly in terms of the rate of substrate use, microbial C-use efficiency, and response to temperature. Substrate mineralization rate increased with temperature with more C being allocated to microbial catabolic rather than anabolic processes. Our results show that climate change is likely to lead to changes in soil organic matter turnover and shift C allocation patterns within the soil microbial community. This is expected to reduce soil quality and exacerbate nutrient losses. Management strategies are required to promote the retention of organic matter in these soils.

Keywords: carbon cycling; groundwater; irrigation; microbial uptake kinetics; substrate-induced respiration; wastewater

1. Introduction

Changing climate, together with increased demand on limited groundwater supplies for agriculture in many arid regions, has led to several national authorities promoting the use of alternative sources of water for crop irrigation (e.g., Saudi Arabia, [1]; California, [2]). Concern for human health has limited its use in commercial food production but in regions experiencing significant water stress, wastewater can contribute approximately 20% of the total irrigation water used [3–6].

In oasis-based agroecosystems, nitrogen (N) represents the key nutrient regulating primary productivity; however, the cycling and competition for N resources in these ecosystems remains poorly understood [7,8]. Recently, it has been discovered that plants can directly compete with microorganisms for both organic (e.g., oligopeptides, amino acids) and inorganic (e.g., NH_4^+ and NO_3^-) forms of N present in soil [9–11]. This challenges the traditional paradigm of nutrient cycling in oasis soils which suggests that plants will only acquire N in an inorganic form. It also highlights the need to better understand how solid soil organic N (SON) and dissolved organic N (DON) cycles within these soils.

DON can enter arid soils from many sources with the quantitative importance of each source highly dependent on management regime, its spatial input pattern (topsoil vs. subsoil, rhizosphere vs. bulk soil),

and its temporal dynamics (e.g., time of day and seasonality) [12]. In oasis ecosystems, a small amount of DON may enter the soil surface from both wet and dry deposition [13], with inputs also occurring from canopy throughfall, especially if spray irrigators are used, from leaf litter [14] or directly in irrigation water or organic residues [7]. In addition, inputs can also occur below-ground from both root and microbial exudation and from root and microbial death [15,16].

The Middle East is already experiencing increasing temperatures due to climate change [17]. Observations in this region record the largest positive annual temperature anomaly outside of polar regions (+2.22 °C) and predictions point towards further increases of between 1.8–4.1 °C by 2050 [18] and increased water scarcity throughout the region [19]. This increase in temperature is likely to impact upon both the availability and quality of water used for irrigating agricultural fields and the intrinsic amount of water present in the soil, which in turn will impact soil microbial activity and the key processes that are mediated by these organisms (e.g., C and N cycling).

DON consists of many individual components ranging from high molecular weight compounds (HMW) such as chlorophyll, deoxyribonucleic acid (DNA), ribonucleic acid (RNA) and proteins through to low molecular weight compounds (LMW) such as, oligopeptides, amino sugars, amino acids, purines and urea [15,20–22]. The subsequent breakdown of HMW DON compounds by microbial exoenzymes is a key bottleneck in the supply of N to plants and microorganisms [9–11,23] and understanding agricultural practices that affect or change exoenzyme activity in oases is key to their better management [24].

To date, relatively little is known about DON and dissolved organic carbon (DOC) cycling in arid soils, particularly in the Middle East. Due to the current and proposed impact of climate change in arid agricultural systems, we need to better understand the factors regulating C and N dynamics in soil with the aim of developing more sustainable agriculture systems in terms of both nutrient and water-use efficiency [18,25]. Consequently, the aim of our research is to expand our fundamental understanding of the effects of temperature on DOC and DON cycling within oasis-based agroecosystems. To enable us to do this, we set objectives to (a) understand the differences in chemical and biological properties of 3 different agricultural soils and their associated irrigation water; (b) use ¹⁴C-labeled DOC and DON to determine the effect of temperature on rates of DOC and DON turnover; and (c) determine the effect of temperature on the microbial partitioning of added DOC and DON substrates. We therefore hypothesized that: (1) mineralization rates of DOC and DON will increase with increasing temperature; (2) the mineralization rate of DON will be higher than for DOC in arid soils due to a greater use of amino acid derived-C in respiratory processes.

2. Material and Methods

2.1. Soil and Water Sampling

Soil and water samples were collected from three agricultural farm sites with contrasting irrigation regimes within the Al-Hassa eastern oasis, Saudi Arabia. Site 1 (25°25.430' N, 49°37.460' E) irrigated its crops with groundwater (GW), Site 2 (25°35.839' N, 49°34.144' E) irrigated with tertiary treated wastewater (TTWW), and Site 3 (25°23.461' N, 49°44.553' E) irrigated with a mixture of groundwater, treated wastewater and farm drainage water (MW). A summary of the main chemical properties of the irrigation water used at each site is presented in Table 1. The dominant crop grown at the three sites was date palms (*Phoenix dactylifera* L.). Each date palm tree is planted at a distance of 4 m × 6 m and interplanted with vegetables, fruit, and Hassawi alfalfa (*Medicago sativa* L.) crops except at Site 2 where they are interplanted with Hassawi alfalfa only. At each site, four independent replicates of topsoil (0–30 cm) and subsoil (30–60 cm) were collected from three separate blocks of 6 m × 6 m using an auger. Each individual field-moist soil sample was placed in an O₂-permeable plastic bag. Additionally, replicate samples of irrigation water ($n = 3$) were collected in clean polypropylene bottles from the pump outlet at each experimental site. All soil and water samples were cooled (4 °C) then immediately shipped to the UK for analysis.

Table 1. Chemical characteristics of the irrigation water types. Values represent means \pm Standard Error of the Mean (SEM) ($n = 3$). Different superscript letters indicate significant differences between irrigation water types ($p \leq 0.05$) and no letters shows there are no significant differences. Electrical Conductivity is indicated as EC.

Water/Irrigation Type	Ground Water	Treated Wastewater	Mixed
Parameters			
pH	7.27 \pm 0.03 ^a	7.22 \pm 0.05 ^a	6.83 \pm 0.04 ^b
EC (mS/cm)	4.92 \pm 0.16 ^b	2.21 \pm 0.03 ^c	7.04 \pm 0.09 ^a
P (mg/L)	0.04 \pm 0.00 ^c	4.99 \pm 0.46 ^a	2.50 \pm 0.11 ^b
Soluble phenolics (mg/L)	1.74 \pm 0.58	1.33 \pm 0.45	3.10 \pm 0.54
NO ₃ ⁻ (mg N/L)	7.02 \pm 0.05 ^b	7.11 \pm 0.22 ^b	9.68 \pm 0.41 ^a
NH ₄ ⁺ (mg N/L)	0.02 \pm 0.01	0.02 \pm 0.00	0.08 \pm 0.04
Dissolved organic N (DON) (mg N/L)	0.41 \pm 0.01 ^b	0.61 \pm 0.09 ^a	0.43 \pm 0.18 ^b
Dissolved organic C (DOC) (mg C/L)	1.03 \pm 0.30 ^c	4.69 \pm 0.36 ^b	6.44 \pm 0.18 ^a
DOC/DON ratio	2.49 \pm 0.70	8.13 \pm 0.87	23.84 \pm 11.65
Amino acids (mg N/L)	0.01 \pm 0.00 ^b	0.05 \pm 0.02 ^a	0.03 \pm 0.00 ^{a,b}

For all three experimental sites the mean annual rainfall is 70 mm, the annual surface irrigation is 2300 mm, and the daily mean air temperatures ranges from 28.0 °C to 47.5 °C (average of 34.1 °C). The highest recorded air temperature is 50 °C. The relative humidity of the air is generally high for arid systems, often reaching 90% in summer [6,26]. The average daily soil temperature in the Al-Hassa eastern oasis typically ranges from 16.4 to 37.9 °C at 20 cm depth and 17.1 to 37.6 °C at 30 cm with an average of 30 °C (Figure 1).

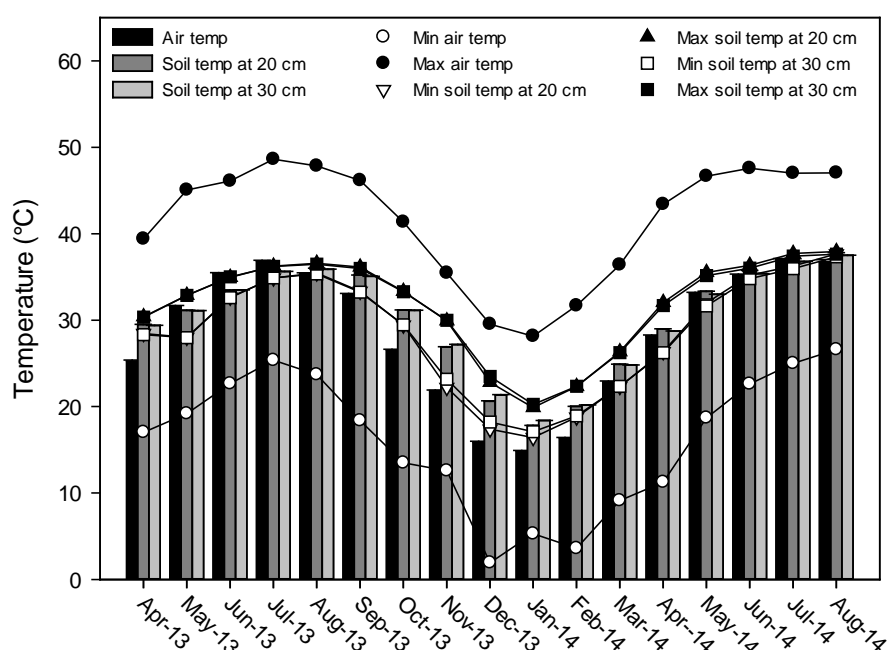


Figure 1. Air temperature and soil temperature at 20 cm and at 30 cm depth in the Al-Hassa oasis from April 2013 to August 2014 (data from Agricultural and Veterinary Training and Research Station, King Faisal University, Al-Hassa, KSA).

2.2. General Soil and Water Characterization

pH and electrical conductivity (EC) were determined by standard electrodes either directly for irrigation water or in 1:2.5 *w/v* soil:distilled water extracts for soil. Soil moisture content was determined gravimetrically by oven-drying (105 °C, 16 h) while organic matter content was determined

by loss-on-ignition (550 °C, 16 h). Soil CaCO₃ was measured by the titration method [27] while soil texture was measured by sedimentation using the Bouyoucos method [27]. Total elemental concentrations were determined by digesting the air-dry soil with 70% HNO₃ (1:4 *w/v*) for 1 h at 100 °C and filtering through a Whatman filter paper No. 541 according to method 3051A [28]. Na was measured using a Model 410 flame photometer (Sherwood Scientific, Cambridge, UK) [27,29] while Mg was measured using a SpectrAA 220FS atomic absorption spectrometer (Varian Inc., Palo Alto, CA, USA). The remaining elements were measured using a S2-Picofox TXRF (Bruker Inc., Billerica, MA, USA). Soil total C, total N and C:N ratio were determined using a CHN2000 analyser (Leco Corp., St Joseph, MI, USA). Fresh soils were extracted with 0.5 M K₂SO₄ (1:5 *w/v*) for determining plant-available P, total extractable phenolics, NO₃⁻, NH₄⁺, protein and free amino acids. Available P, phenol, NO₃⁻, NH₄⁺, and protein were measured colorimetrically using a Powerwave XS spectrophotometer (Biotek Instruments Inc., Winooski, VT, USA). Available P was measured using the ammonium molybdate-H₂SO₄-ascorbic acid method of [30]. Phenolics were measured using the Folin-Ciocalteu reagent in the presence of sodium carbonate [31], NO₃⁻ by reaction with VCl₃ and N-(1-naphthyl)ethylenediamine dihydrochloride [32]. NH₄⁺ was determined using the sodium salicylate-sodium nitroprusside-hypochlorite method of [33]. The Bradford method was used to estimate protein content [34]. Total free amino acids were determined by fluorescence according to [35] while DON and DOC were determined using a Multi-N/C 2100 S TOC/TN analyzer (Analytik-Jena AG, Jena, Germany). Microbial biomass C and N were determined by the 7 day chloroform fumigation-0.5 M K₂SO₄ extraction procedure of [11] ($K_{EN} = 0.5$; $K_{EC} = 0.35$). Basal soil respiration (SR) was measured using an automated CIRAS-SC soil respirometer at 20 °C (PP Systems Ltd., Hitchin, UK).

2.3. Soil Phospholipid Fatty Acid (PLEA) Microbial Community Structure

Microbial community structure was measured by phospholipid fatty acid (PLFA) analysis following the method of [36]. Briefly, replicate samples of soil from each site were sieved to pass 5 mm, stored, and shipped on dry ice (-78.5 °C) to a commercial laboratory (Microbial ID, Newark, DE, USA), for analysis. Samples (2 g) were then freeze-dried and Bligh-Dyer extractant (4.0 mL) containing an internal standard added. Tubes were sonicated in an ultrasonic cleaning bath for 10 min at room temperature before rotating end-over-end for 2 h. After centrifuging (10 min), the liquid phase was transferred to clean 13 mm × 100 mm screw-cap test tubes and 1.0 mL each of chloroform and water added. The upper phase was removed by aspiration and discarded while the lower phase, containing the extracted lipids, was evaporated at 30 °C. Lipid classes were separated by solid phase extraction (SPE) using a 96-well SPE plate containing 50 mg of silica per well (Phenomenex, Torrance, CA, USA). Phospholipids were eluted with 0.5 mL of 5:5:1 methanol:chloroform:H₂O [37] into glass vials, the solution evaporated (70 °C, 30 min). Trans esterification reagent (0.2 mL) was added to each vial, the vials sealed and incubated (37 °C, 15 min). Acetic acid (0.075 M) and chloroform (0.4 mL each) were then added. The chloroform was evaporated just to dryness and the samples dissolved in hexane. An Agilent 6890 gas chromatograph (GC) (Agilent Technologies, Wilmington, DE, USA) equipped with auto sampler, split-split less inlet, and flame ionization detector was used. Fatty acid methyl esters (FAMES) were separated on an Agilent Ultra 2 column, 25 m long × 0.2 mm internal diameter × 0.33 μm film thickness. FAMES were identified using the MIDI PLFAD1 calibration mix (Microbial ID, Inc., Newark, DE, USA) and classified according to [38]. The biomarker group for putative arbuscular mycorrhizal fungi (AM Fungi) was 16:1ω5c, for Gram-negative bacteria they were 18:1ω7c, 17:0cy and 19:0cy, while for Gram-positive bacteria they were 15:0i, 15:0a, 16:0i, 17:0i and 17:0a. The biomarker used for eukaryotes was 20:4ω6c, for total fungi it was 18:2ω6c, and for actinomycetes they were 16:0 10-Me, 17:0 10-Me and 18:0 10-Me) [39].

2.4. Rate of ¹⁴C-Labelled Substrate Mineralization in Soil

Replicate samples of soil from each site (10 g) were placed in individual 50 mL sterile polypropylene tubes and 0.5 mL of a ¹⁴C-uniformly labelled substrate (10 μM; 3.7 kBq mL⁻¹) was

added to the soil surface. The ^{14}C -labelled substrate added to individual tubes included: (i) glucose, (ii) an equimolar mixture of 15 different L-amino acids (alanine, arginine, aspartic acid, leucine, tyrosine, valine, phenylalanine, glutamic acid, threonine, proline, lysine, histidine, glycine, isoleucine, serine), or (iii) the oligopeptide L-trialanine (a component of peptidoglycan). After addition of the ^{14}C -labelled substrate, a 1 M NaOH trap (1 mL) was placed inside each tube to catch respired $^{14}\text{CO}_2$ and the tubes sealed and incubated at either 10, 20, 30 or 40 °C. Production of $^{14}\text{CO}_2$ over time was measured by periodically replacing the NaOH trap after 0.5, 1, 3, 6, 24, 48, 168, 336, 504, and 672 h. $^{14}\text{CO}_2$ was determined by liquid scintillation counting using a Wallac 1409 liquid scintillation counter (PerkinElmer Inc., Waltham, MA, USA) and OptiPhase Hi-safe 3 scintillation cocktail (PerkinElmer Inc.). After the removal of the final NaOH trap at 28 d, the soils were shaken for 20 min at 200 rev min^{-1} with 25 mL of 0.5 M K_2SO_4 to extract any ^{14}C remaining in solution or bound to the soil's solid phase [23,40]. The extracts were measured by liquid scintillation counting as described earlier. Near identical experiments were also performed but with sterilized soil (autoclaved at 121 °C, 1 h and cooled for 10 min prior to use) to confirm that the release of $^{14}\text{CO}_2$ was biologically mediated and not produced from abiotic processes. The rate of ^{14}C -substrate mineralization in the soil was described by a double first-order exponential decay model:

$$f = [a_1 \times \exp(-k_1 t)] + [a_2 \times \exp(-k_2 t)] \quad (1)$$

where f is the percentage of ^{14}C -substrate remaining in the soil at time t (hours). Parameters a_1 and a_2 represent the size (% of total ^{14}C added) of the fast and slow ^{14}C turnover pools respectively [22,41]. k_1 is the rate constant describing the turnover rate of C pool a_1 which is ascribed to the immediate use of substrate-derived ^{14}C in catabolic processes (i.e., respiration). k_2 is the rate constant describing the turnover of C pool a_2 and is attributed to the second slower phase of $^{14}\text{CO}_2$ production associated with turnover of substrate-derived ^{14}C immobilised in the microbial biomass [41]. The half-life ($t_{\frac{1}{2}}$) of pool a_1 is defined as:

$$t_{\frac{1}{2}} = \ln(2)/k_1 \quad (2)$$

Total microbial uptake ($^{14}\text{C}_{\text{uptake}}$) can be defined as:

$$^{14}\text{C}_{\text{uptake}} = ^{14}\text{C}_{\text{Tot}} - ^{14}\text{C}_{\text{K}_2\text{SO}_4} \quad (3)$$

where $^{14}\text{C}_{\text{Tot}}$ is the total amount of ^{14}C label added to the soil and $^{14}\text{C}_{\text{K}_2\text{SO}_4}$ is the amount of ^{14}C label recovered in the K_2SO_4 extract [23]. The amount of labelled ^{14}C remaining in the microbial biomass ($^{14}\text{C}_{\text{mic}}$) after 28 days was calculated as follows:

$$^{14}\text{C}_{\text{mic}} = ^{14}\text{C}_{\text{Tot}} - ^{14}\text{CO}_2 - ^{14}\text{C}_{\text{K}_2\text{SO}_4} \quad (4)$$

where $^{14}\text{CO}_2$ is the total amount of label recovered in the NaOH traps [23]. Lastly, microbial C use efficiency (Mic_{eff}) for each substrate can be defined as, [41,42].

$$\text{Mic}_{\text{eff}} = a_2 / (a_1 + a_2) \quad (5)$$

2.5. Effects of Temperature on ^{14}C Mineralization Rate

The effect of temperature (T) on ^{14}C mineralization rate (MR) was described by applying a square root transformation model to the data according to [43,44] using the equation

$$MR^{\frac{1}{2}} = \alpha (T - T_{\text{min}}) \quad (6)$$

where MR is the mineralization rate (defined as the initial linear rate of $^{14}\text{CO}_2$ production at each temperature), α is a slope parameter linked to the absolute rates, and T_{min} is the temperature at which

mineralization ceases. The linear phase of ^{14}C evolution was defined as 0–48 h at 10 °C, 0–24 h at 20 °C, 0–6 h at 30 °C, and 0–3 h at 40 °C.

2.6. Statistical Analysis

After testing for normality, statistical analyses (analysis of variance (ANOVA) with Tukey's pairwise comparison) were performed using SPSS 20 (SPSS Inc., Chicago, IL, USA) or Minitab 16 (Minitab Inc., State College, PA, USA) with significance differences set at $p \leq 0.05$ unless otherwise stated. The double first-order exponential decay equation was fitted to experimental results using Sigmaplot 12.3 (SPSS Inc., Chicago, IL, USA). Linear regression models describing ^{14}C mineralization rate and temperature were made using Sigmaplot 12.3.

3. Results

3.1. General Physical and Chemical Irrigation Water and Soil Properties

The chemical properties of irrigation water used at each site are presented in Table 1 and additional material in Table S1. All chemical characteristics were within acceptable national values of water quality for irrigation according to [45,46] with the exception of the EC value of groundwater and mixed water, which were higher than the standard of 3 mS cm^{-1} . There were significant differences between all chemical characteristics of irrigation waters except Cr, Fe, phenolics, total N, total C, NH_4^+ , and DOC/DON ratio content. Groundwater showed the highest pH and Zn contents, but the lowest available P, NO_3^- , DON, DOC, and amino acid contents of the three irrigation water sources. Treated wastewater showed the highest available P, DON, and amino acid contents; however, it shows the lowest EC, Na, S, Cl, K, Ca, Mg, and Zn contents of the three irrigation water sources. The mixed water showed the highest EC, Na, S, Cl, K, Ca, Mg, NO_3^- , and DOC contents but showed the lowest pH value of the three irrigation water sources.

Physical and chemical characteristics of the soils used in this study are presented in Tables 2 and 3. Soils were classified as sand or sandy loam [47]; the average pH and EC values for all soils were 8.55 ± 0.02 and $0.72 \pm 0.08 \text{ mS cm}^{-1}$, respectively. No differences in soil pH and EC were observed between sites or sampling depths. The soils tested in this study can be classified as having low to medium organic matter (OM) contents, according to [48]; the average OM and CaCO_3 contents for all soils were $1.7\% \pm 0.22\%$ and $23.6\% \pm 3.02\%$, respectively. Significant differences in OM and CaCO_3 were observed between sites ($p \leq 0.05$), but no significant differences were observed between sampling depths, except in OM contents of site 1. In topsoils, the highest total C (TC) content was observed in site 3, in the subsoils; the highest content was shown in site 2 ($23.6 \pm 2.8 \text{ g C kg}^{-1}$ soil, and $34.5 \pm 3.6 \text{ g C kg}^{-1}$ soil in topsoils and subsoils, respectively); the lowest TC content was observed in site 1 in both topsoils and subsoils ($13.3 \pm 1.3 \text{ g C kg}^{-1}$ soil, and $10.5 \pm 1.4 \text{ g C kg}^{-1}$ soil in topsoils and subsoils, respectively) with significant differences between sites ($p \leq 0.05$), but no significant differences between sampling depths ($p > 0.05$). The average total N (TN) contents and C:N ratio for all soils were $0.94 \pm 0.07 \text{ g N kg}^{-1}$ soil and 22.0 ± 4.8 , respectively. No differences were observed between sites or sampling depths, but there were significant differences between sites in the subsoil C:N ratios. All soils possessed a very low NO_3^- content, according to [49]. The highest NO_3^- concentration was shown in site 2 ($7.7 \pm 0.6 \text{ mg NO}_3^- \text{-N kg}^{-1}$ soil, and $3.2 \pm 0.6 \text{ mg NO}_3^- \text{-N kg}^{-1}$ soil in topsoils and subsoils, respectively) and the lowest NO_3^- concentration in site 1 ($4.6 \pm 0.6 \text{ mg NO}_3^- \text{-N kg}^{-1}$ soil, and $0.7 \pm 0.1 \text{ mg NO}_3^- \text{-N kg}^{-1}$ soil in topsoils and subsoils, respectively), with significant differences between sites ($p \leq 0.05$), but no significant differences between sampling depth, except in site 1. Site 1 showed the highest NH_4^+ concentration in top and subsoils ($1.05 \pm 0.13 \text{ mg NH}_4^+ \text{-N kg}^{-1}$ soil and $1.3 \pm 0.2 \text{ mg NH}_4^+ \text{-N kg}^{-1}$ soil, respectively), while the lowest NH_4^+ concentration in the topsoils was observed in site 2; in the subsoils, the lowest content was observed in site 3 ($0.05 \pm 0.02 \text{ mg NH}_4^+ \text{-N kg}^{-1}$ soil, and $0.33 \pm 0.18 \text{ mg NH}_4^+ \text{-N kg}^{-1}$ soil, respectively) with significant differences between sites ($p \leq 0.05$), but no significant differences between sampling depths ($p > 0.05$). Total free amino

acid (TFAA) concentrations show similar patterns to NH_4^+ but no significant differences exist between sites or sampling depths ($p > 0.05$), except between the depths in site 1 ($0.19 \pm 0.01 \text{ mg TFAA-N kg}^{-1}$ soil, and $0.13 \pm 0.01 \text{ mg TFAA-N kg}^{-1}$ soil in topsoils and subsoils, respectively). As expected, TFAA concentrations were lower than DON concentrations in all sites and followed the pattern: site 2 > site 3 \geq site 1, with significant differences between them ($p \leq 0.05$). The average protein, DON, DOC, microbial N and microbial C content for all soil sites were $4.17 \pm 0.35 \text{ mg N kg}^{-1}$ soil, $6.73 \pm 0.62 \text{ mg N kg}^{-1}$ soil, $41.0 \pm 5.5 \text{ mg C kg}^{-1}$ soil, $10.7 \pm 2.8 \text{ mg N kg}^{-1}$ soil, and $105.2 \pm 15.2 \text{ mg C kg}^{-1}$ soil, respectively. No differences were observed between sites or sampling depths, except between sites in the subsoils and DOC concentrations, and followed the pattern of site 3 > site 2 \geq site 1 between sites in the topsoils and microbial N, and followed the pattern of site 2 > site 3 > site 1 between sampling depths and microbial N or C in site 2 ($p \leq 0.05$). TFAA concentrations represent 2.44% of DON concentrations in topsoils and 2.03% in subsoils, following a pattern of site 1 > site 2 > site 3. DOC/DON ratio showed that there were significant differences between sites in the subsoils, following a pattern of site 3 \geq site 1 > site 2 (5.70 ± 0.65 , 5.33 ± 0.29 , and 3.25 ± 0.21 respectively) ($p \leq 0.05$), but there were no significant differences between sites in the topsoils or sampling depths ($p > 0.05$), except between the sampling depths in site 2 ($p \leq 0.05$).

Table 2. Physical, biological and chemical characteristics of the soils used in the experiments. Values represent mean \pm SEM ($n = 3$). Significant differences between depths are indicated by * = $p \leq 0.05$ and different lower case letters identify significant differences between sites ($p \leq 0.05$) in topsoil. No letters shows there are no significant differences.

Soil/Irrigation Type	Site 1	Site 2	Site 3
Parameter	(0–30 cm)	(0–30 cm)	(0–30 cm)
pH	8.51 ± 0.03	8.66 ± 0.02	8.56 ± 0.07
Electrical conductivity (mS/cm)	0.91 ± 0.07	0.40 ± 0.02	0.67 ± 0.15
Moisture content (%)	12.8 ± 0.3^b	* 12.7 ± 0.7^b	18.2 ± 0.6^a
Organic matter (%)	* 1.26 ± 0.05^b	$1.56 \pm 0.06^{a,b}$	2.65 ± 0.23^a
CaCO ₃ (%)	23.5 ± 0.8^b	27.9 ± 2.1^a	15.0 ± 2.4^c
Soil texture	Sand	Sand	Sandy loam
Na (g/kg)	0.56 ± 0.15	0.32 ± 0.06	0.49 ± 0.11
Al (g/kg)	* 1.47 ± 0.04^a	0.60 ± 0.08^b	$1.32 \pm 0.31^{a,b}$
S (g/kg)	0.20 ± 0.02	0.04 ± 0.02	0.09 ± 0.04
Cl (g/kg)	* 0.25 ± 0.02	0.21 ± 0.02	0.25 ± 0.07
K (g/kg)	* $0.70 \pm 0.01^{a,b}$	0.58 ± 0.04^b	0.93 ± 0.13^a
Ca (g/kg)	* 33.0 ± 0.7	37.7 ± 2.3	37.6 ± 4.3
Mg (g/kg)	3.05 ± 0.10^b	3.46 ± 0.34^b	9.25 ± 1.17^a
Mn (g/kg)	* 0.06 ± 0.00	0.05 ± 0.01	0.08 ± 0.01
Fe (g/kg)	* 1.93 ± 0.03^b	1.40 ± 0.11^c	2.64 ± 0.27^a
Zn (g/kg)	0.02 ± 0.00	0.02 ± 0.01	0.02 ± 0.00
Total C (g C/kg)	13.2 ± 1.3^b	21.6 ± 1.9^a	23.6 ± 2.8^a
Total N (g N/kg)	1.00 ± 0.06	0.83 ± 0.04	1.19 ± 0.08
Total C:N ratio	13.6 ± 1.3	27.9 ± 5.5	20.5 ± 3.0
NO ₃ [−] (mg N/kg)	* 4.60 ± 0.55^b	7.67 ± 0.55^a	4.84 ± 0.45^b
NH ₄ ⁺ (mg N/kg)	1.05 ± 0.13^a	0.05 ± 0.02^b	0.11 ± 0.18^b
Amino acids (mg N/kg)	* 0.19 ± 0.01	0.15 ± 0.02	0.17 ± 0.03
Protein (mg N/kg)	5.28 ± 0.37	2.53 ± 0.32	4.83 ± 0.59
DON (mg N/kg)	5.91 ± 0.78	6.91 ± 1.12	9.64 ± 2.75
DOC (mg C/kg)	35.0 ± 6.6	39.6 ± 8.6	66.5 ± 23.4
Microbial N (mg N/kg)	8.88 ± 0.65^b	* 20.2 ± 1.4^a	18.5 ± 4.8^a
Microbial C (mg C/kg)	109 ± 16	* 172 ± 7	127 ± 31
DOC/DON ratio	5.90 ± 0.84	* 5.81 ± 0.21	12.05 ± 5.97
Phenolics (mg/kg)	* 5.73 ± 0.12	6.64 ± 2.02	* 4.69 ± 1.30
Available P (mg P/kg)	* 10.0 ± 1.8	41.5 ± 3.3	* 35.7 ± 2.0
Soil respiration ($\mu\text{g CO}_2/\text{g/h}$)	* 0.12 ± 0.01	0.14 ± 0.01	0.16 ± 0.01

Table 3. Physical, biological and chemical characteristics of the subsoil used in the experiments. Values represent mean \pm SEM ($n = 3$). Different lowercase letters identify significant differences between sites ($p \leq 0.05$) in subsoil. No letters shows there are no significant differences.

Soil/Irrigation Type	Site 1	Site 2	Site 3
Parameter	(30–60 cm)	(30–60 cm)	(30–60 cm)
pH	8.51 \pm 0.06	8.51 \pm 0.01	8.55 \pm 0.07
Electrical conductivity (mS/cm)	0.95 \pm 0.14	0.59 \pm 0.03	0.81 \pm 0.15
Moisture content (%)	13.4 \pm 0.4 ^c	27.1 \pm 1.1 ^a	20.3 \pm 0.5 ^b
Organic matter (%)	0.89 \pm 0.04 ^c	1.80 \pm 0.05 ^b	2.05 \pm 0.23 ^a
CaCO ₃ (%)	25.6 \pm 1.7 ^{a,b}	35.5 \pm 3.3 ^a	14.1 \pm 2.4 ^b
Soil texture	Sand	Sandy loam	Sandy loam
Na (g/kg)	0.42 \pm 0.17	0.51 \pm 0.06	0.53 \pm 0.06
Al (g/kg)	0.68 \pm 0.09	0.41 \pm 0.04	0.71 \pm 0.20
S (g/kg)	0.04 \pm 0.04	0.03 \pm 0.01	0.08 \pm 0.02
Cl (g/kg)	0.14 \pm 0.01 ^b	0.18 \pm 0.00 ^{a,b}	0.21 \pm 0.01 ^a
K (g/kg)	0.49 \pm 0.03 ^b	0.50 \pm 0.02 ^b	0.98 \pm 0.08 ^a
Ca (g/kg)	21.6 \pm 1.0 ^b	38.5 \pm 2.5 ^a	37.1 \pm 2.4 ^a
Mg (g/kg)	2.58 \pm 0.15 ^c	4.32 \pm 0.17 ^b	8.47 \pm 1.44 ^a
Mn (g/kg)	0.04 \pm 0.00 ^b	0.05 \pm 0.00 ^b	0.07 \pm 0.01 ^a
Fe (g/kg)	1.25 \pm 0.07 ^b	1.36 \pm 0.09 ^b	2.69 \pm 0.23 ^a
Zn (g/kg)	0.01 \pm 0.00	0.01 \pm 0.00	0.01 \pm 0.00
Total C (g C/kg)	10.5 \pm 1.4 ^b	34.5 \pm 3.6 ^b	22.8 \pm 2.8 ^a
Total N (g N/kg)	0.81 \pm 0.12	0.74 \pm 0.03	1.07 \pm 0.08
Total C:N ratio	13.9 \pm 1.0 ^b	48.2 \pm 5.5 ^b	22.1 \pm 3.0 ^b
NO ₃ ⁻ (mg N/kg)	0.69 \pm 0.09 ^b	3.22 \pm 0.62 ^b	1.04 \pm 0.45 ^b
NH ₄ ⁺ (mg N/kg)	1.29 \pm 0.22 ^a	0.38 \pm 0.11 ^b	0.33 \pm 0.18 ^b
Amino acids (mg N/kg)	0.13 \pm 0.01	0.10 \pm 0.01	0.12 \pm 0.02
Protein (mg N/kg)	4.07 \pm 0.34	4.02 \pm 0.69	4.28 \pm 0.25
DON (mg N/kg)	4.67 \pm 0.44	6.92 \pm 1.69	6.30 \pm 0.80
DOC (mg C/kg)	25.1 \pm 3.7 ^b	30.7 \pm 7.6 ^{a,b}	48.6 \pm 2.3 ^a
Microbial N (mg N/kg)	1.09 \pm 0.23	5.5 \pm 0.7	10.5 \pm 5.7
Microbial C (mg C/kg)	59 \pm 11	92 \pm 5	74 \pm 40
DOC/DON ratio	5.33 \pm 0.29 ^a	3.25 \pm 0.21 ^b	5.70 \pm 0.65 ^a
Phenolics (mg/kg)	4.03 \pm 0.06	6.55 \pm 2.57	0.96 \pm 0.25
Available P (mg P/kg)	3.0 \pm 0.8	19.2 \pm 2.5	4.9 \pm 2.0
Soil respiration (μ g CO ₂ /g/h)	0.09 \pm 0.00 ^b	0.12 \pm 0.02 ^{a,b}	0.15 \pm 0.01 ^a

3.2. Soil PLFA Microbial Community Structure

Soil PLFA microbial community structure is presented in Figure 2. The average microbial biomass based on total PLFA was 45.9 ± 11.1 and 25.6 ± 4.1 nmol g⁻¹ in topsoils and subsoils, respectively. In most soils, the presence of the PLFAs followed the series: Gram-negative bacteria > Gram-positive bacteria > actinomycetes > arbuscular mycorrhiza (AM) fungi \geq fungi \geq eukaryotes. Overall, few major differences were observed in the PLFA composition between sites or sampling depths.

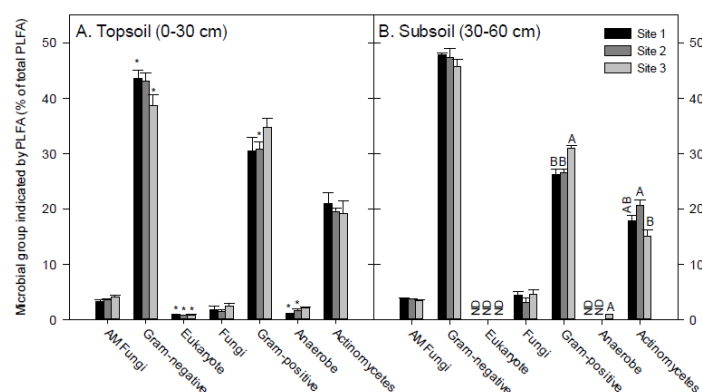


Figure 2. Soil PLFA microbial community structure in topsoils (Panel A) and subsoils (Panel B) from three agricultural oasis sites. Values represent means \pm SEM ($n = 3$). ND indicates not detected. Different letters identify significant differences between sites ($p \leq 0.05$), * indicate significant differences between depths, and no letters shows there are no significant differences.

3.3. Dissolved Organic Nitrogen (DON) Compounds' Mineralization and Half-Life

Overall, no significant differences were observed between the goodness of fit of the double exponential decay model to the experimental data ($R^2 = 0.999 \pm 0.001$) when comparing different substrates or sites at different temperatures. The effect of temperature on different ^{14}C -substrate mineralization in the topsoils and subsoils are shown in Figures 3 and 4 respectively, while the kinetic parameters from the double first-order exponential decay equation in different sites are presented in Tables 4 and 5. There were no significant effects observed between sites or sampling depths with the production of $^{14}\text{CO}_2$ ($p > 0.05$). The production of $^{14}\text{CO}_2$ increases with increasing temperature in almost all cases ($p \leq 0.05$), as shown in Figures 3 and 4. The cumulative amount of $^{14}\text{CO}_2$ evolved after the addition of glucose to the topsoils and subsoils increased significantly with increasing temperature from 20 °C to 30 °C for all soils, with the pattern showing little difference between sites. Although temperature increases overall mineralization, increasing temperatures from 30 °C to 40 °C for all soils and substrates had little overall effect on the final amount of ^{14}C -substrate mineralized (Figures 3 and 4).

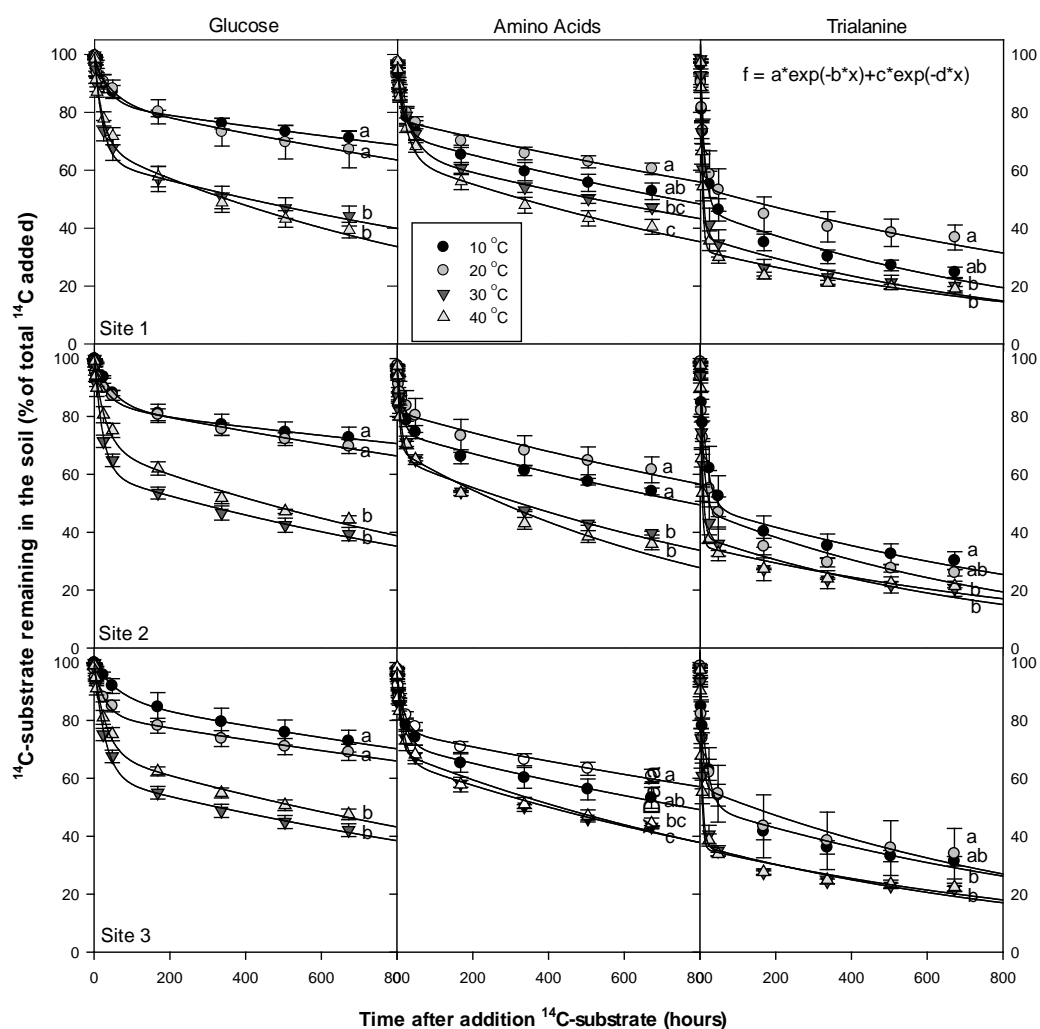


Figure 3. Temperature-dependent mineralization of three different ^{14}C -labelled substrates in topsoils (0–30 cm) collected from three agricultural oasis sites. Points represent means \pm SEM ($n = 3$). Different letters indicate significant differences between temperatures ($p \leq 0.05$). The legend is the same for all panels. The substrates are arranged vertically and the sites horizontally within the panels.

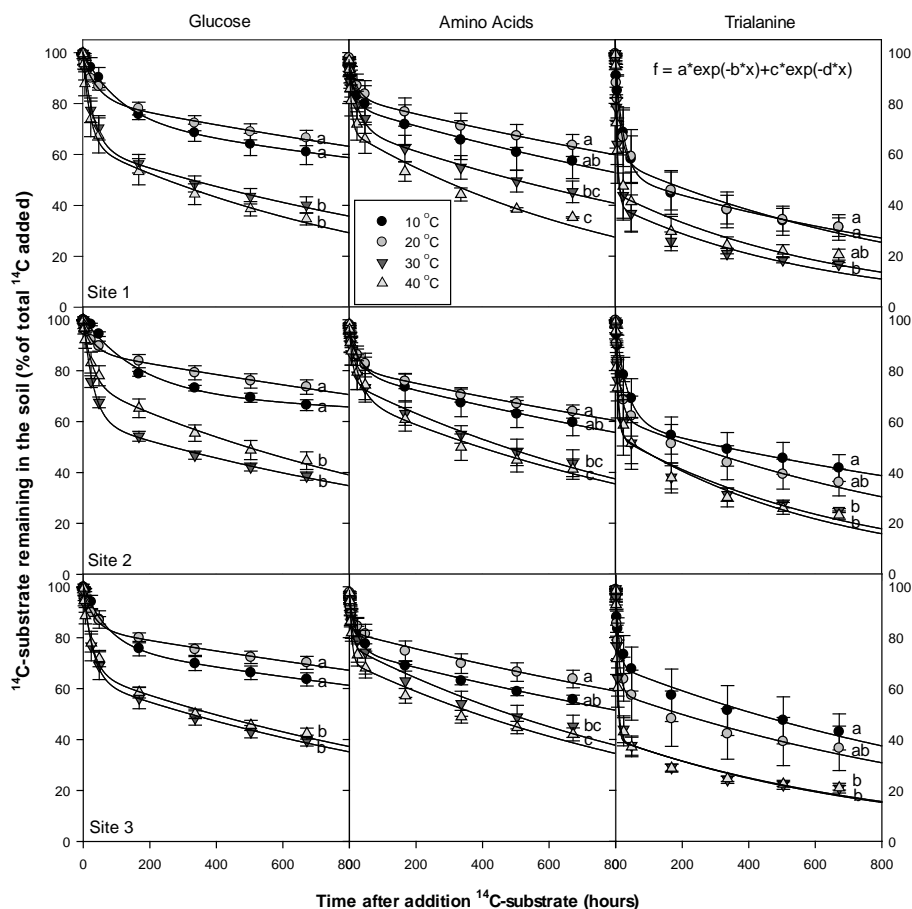


Figure 4. Temperature-dependent mineralization of three different ¹⁴C-labelled substrates in subsoils (30–60 cm) collected from three agricultural oasis sites. Points represent means ± SEM (*n* = 3). Different letters indicate significant differences between temperatures (*p* ≤ 0.05). The legend is the same for all panels. The substrates are arranged vertically and the sites horizontally within the panels.

Table 4. Influence of soil temperature on the modelled kinetic parameters describing the rapid phase of turnover of ¹⁴C-labelled glucose, amino acids, and trialanine in the topsoils of three different agriculture sites. Values represent mean ± SEM (*n* = 3). Different letters indicate significant differences between temperatures (*p* ≤ 0.05), while no letters indicate there are no significant differences.

Sites	Temperature (°C)	Top Soils (0–30 cm)		
		Glucose (%)	Amino Acids (%)	Trialanine (%)
Pool <i>a</i> ₁				
Site 1	10	19.1 ± 2.7 ^b	21.9 ± 2.2 ^{b,c}	50.2 ± 3.2 ^{b,c}
	20	17.9 ± 3.6 ^b	20.1 ± 1.8 ^c	45.6 ± 4.9 ^c
	30	36.6 ± 7.2 ^a	29.0 ± 1.2 ^{a,b}	66.3 ± 6.8 ^{a,b}
	40	29.2 ± 2.7 ^{a,b}	31.2 ± 2.6 ^a	70.7 ± 4.5 ^a
Site 2	10	18.2 ± 4.0 ^{b,c}	21.0 ± 1.9 ^b	48.3 ± 4.3 ^b
	20	13.0 ± 1.3 ^c	17.8 ± 4.0 ^b	54.6 ± 4.9 ^{a,b}
	30	41.4 ± 2.0 ^a	32.6 ± 0.4 ^a	66.0 ± 6.9 ^a
	40	28.8 ± 3.8 ^b	30.5 ± 0.9 ^a	70.0 ± 1.5 ^a
Site 3	10	40.8 ± 2.1	22.9 ± 2.4 ^b	45.0 ± 2.1 ^b
	20	16.0 ± 2.1	20.0 ± 1.8 ^b	46.1 ± 7.3 ^b
	30	41.1 ± 2.1	30.2 ± 0.6 ^a	66.9 ± 2.6 ^a
	40	30.4 ± 1.0	30.9 ± 2.2 ^a	68.5 ± 1.5 ^a

Table 4. Cont.

		Pool a_2			
Site 1	10	81.13 ± 2.66 ^b	72.57 ± 2.39 ^{b,c}	45.47 ± 3.05 ^{b,c}	
	20	79.15 ± 4.41 ^b	77.24 ± 1.88 ^c	51.91 ± 5.05 ^c	
	30	64.69 ± 6.73 ^a	65.61 ± 1.90 ^{a,b}	37.09 ± 5.09 ^{a,b}	
	40	68.47 ± 2.86 ^{a,b}	64.12 ± 3.46 ^a	32.23 ± 2.43 ^a	
Site 2	10	82.03 ± 4.20 ^{b,c}	74.40 ± 1.84 ^b	49.27 ± 3.82 ^b	
	20	84.63 ± 1.59 ^c	79.36 ± 3.91 ^b	43.74 ± 2.76 ^{a,b}	
	30	60.08 ± 1.85 ^a	63.80 ± 1.30 ^a	36.52 ± 4.15 ^a	
	40	70.72 ± 4.95 ^b	68.33 ± 0.67 ^a	35.20 ± 1.09 ^a	
Site 3	10	58.99 ± 21.48	71.71 ± 2.98 ^b	50.71 ± 2.28 ^b	
	20	81.60 ± 2.35	76.72 ± 1.93 ^b	53.69 ± 5.69 ^b	
	30	60.05 ± 2.02	66.47 ± 0.37 ^a	36.36 ± 1.80 ^a	
	40	68.54 ± 1.06	67.52 ± 1.34 ^a	35.73 ± 0.87 ^a	

Table 5. Influence of soil temperature on the modelled kinetic parameters describing the rapid phase of turnover of ¹⁴C-labelled glucose, amino acids, and trialanine in the subsoils of three different agriculture sites. Values represent mean ± SEM ($n = 3$). Different letters indicate significant differences between temperatures ($p \leq 0.05$), while no letters indicate there are no significant differences.

Sites	Temperature (°C)	Sub Soils (30–60 cm)		
		Glucose (%)	Amino Acids (%)	Trialanine (%)
Pool a_1				
Site 1	10	33.7 ± 9.0	16.5 ± 5.8	46.3 ± 7.1
	20	17.0 ± 2.6	14.5 ± 4.0	46.1 ± 8.0
	30	38.4 ± 5.2	23.5 ± 4.4	66.6 ± 9.3
	40	37.2 ± 6.2	31.0 ± 3.5	68.6 ± 9.9
Site 2	10	31.0 ± 4.5 ^b	17.0 ± 4.2 ^b	38.9 ± 7.0
	20	11.7 ± 2.0 ^c	15.9 ± 2.0 ^b	40.1 ± 6.3
	30	42.0 ± 1.7 ^a	25.2 ± 3.4 ^{a,b}	51.7 ± 7.4
	40	25.3 ± 1.7 ^b	29.5 ± 1.6 ^a	52.6 ± 10.6
Site 3	10	25.2 ± 1.7 ^b	19.4 ± 1.2	32.5 ± 8.3 ^b
	20	14.8 ± 1.4 ^c	16.4 ± 3.4	42.1 ± 9.9 ^{a,b}
	30	38.2 ± 3.9 ^a	33.2 ± 7.5	65.0 ± 5.4 ^a
	40	33.2 ± 0.8 ^{a,b}	30.3 ± 3.3	65.4 ± 5.9 ^a
Pool a_2				
Site 1	10	66.96 ± 8.61	78.90 ± 6.76	52.32 ± 7.70
	20	81.13 ± 2.90	82.13 ± 4.87	53.82 ± 6.93
	30	63.31 ± 4.51	70.71 ± 3.70	38.01 ± 6.60
	40	64.01 ± 5.97	66.39 ± 3.77	37.03 ± 5.19
Site 2	10	69.61 ± 4.48 ^b	78.77 ± 5.01 ^b	59.70 ± 7.56
	20	87.28 ± 2.39 ^c	80.76 ± 2.57 ^b	60.34 ± 6.51
	30	60.06 ± 1.72 ^a	72.15 ± 2.85 ^{a,b}	48.57 ± 5.25
	40	75.22 ± 1.25 ^b	68.66 ± 1.79 ^a	48.54 ± 7.78
Site 3	10	75.20 ± 1.72 ^b	75.52 ± 1.45	65.34 ± 10.05 ^b
	20	83.25 ± 1.79 ^c	80.98 ± 4.15	56.89 ± 10.09 ^{a,b}
	30	62.94 ± 3.68 ^a	63.20 ± 6.87	39.23 ± 3.67 ^a
	40	66.97 ± 0.46 ^{a,b}	66.19 ± 2.06	39.02 ± 3.74 ^a

The shortest half-life ($t_{\frac{1}{2}}$) of the fast mineralization pool (a_1) of glucose in both topsoils and subsoils was observed in site 1 (11.7 ± 3.7 h and 18.4 ± 8.5 h, respectively). Amino acid $t_{\frac{1}{2}}$ was shortest in topsoils of site 2 and subsoils of site 3 (4.4 ± 0.5 h; 9.1 ± 5.1 h, respectively). The shortest $t_{\frac{1}{2}}$ of

trialanine was observed in topsoil of site 2 and subsoil of site 3 (2.9 ± 0.3 h; 4.2 ± 1.3 h, respectively). There were no significant differences in $t_{\frac{1}{2}}$ between sites, except after the addition of amino acids at 40 °C, which led to significant differences between sites in topsoil and followed the pattern of site 1 > site 3 > site 2. In most cases, topsoils exhibited shorter $t_{\frac{1}{2}}$ values than subsoils, with $t_{\frac{1}{2}}$ values decreasing with increasing temperature with some significant differences apparent (Table 6). The pool size a_1 describes the relative amount of ^{14}C substrates taken up and used immediately in respiratory processes by the microbial community. In all cases, no significant effects were observed between sites or sampling depths in the size of pool a_1 ($p > 0.05$), but temperature generally increased the amount of ^{14}C allocated to pool a_1 . Increasing temperatures from 20 °C to 30 °C for all soils and substrates has some overall effect on the size of pool a_1 and a_2 ($p \leq 0.05$; Tables 4 and 5). Increasing temperatures from 30 °C to 40 °C for all sites after the addition of ^{14}C amino acids or ^{14}C trialanine has some overall effect on the size of pool a_1 and a_2 ($p \leq 0.05$). The only exception was an observed decrease in C allocation to pool a_1 after the addition of ^{14}C amino acids to the topsoil of site 2 and the subsoil of site 3 when temperature increased from 30 °C to 40 °C; allocation to pool a_2 consequently increased. ^{14}C partitioned into pool a_1 after the addition of ^{14}C glucose decreased in both topsoil and subsoils, with increasing temperature from 30 °C to 40 °C in all soil types. Only a small amount of unmetabolized ^{14}C label was recovered from the soil by 0.5 M K_2SO_4 at the end of 28 day incubation periods (<1% of the total ^{14}C applied in almost all cases).

Table 6. Influence of soil temperature on half-life values of substrates in topsoil and subsoil of three different agriculture sites. Values represent mean \pm SEM ($n = 3$). Different letters indicate significant differences between temperatures ($p \leq 0.05$), while no letters indicate there are no significant differences.

		Glucose (h)	Amino Acids (h)	Trialanine (h)
Half-life ($t_{\frac{1}{2}}$) of Pool a_1				
Topsoil Site 1	10	33.3 \pm 22.5 ^{a,b}	12.9 \pm 3.9 ^{a,b}	9.0 \pm 2.8
	20	71.9 \pm 27.6 ^a	5.6 \pm 0.7 ^b	8.6 \pm 4.3
	30	11.7 \pm 3.7 ^{a,b}	25.0 \pm 6.7 ^a	4.0 \pm 0.4
	40	15.9 \pm 1.3 ^b	16.3 \pm 1.8 ^{a,b}	3.4 \pm 0.5
Topsoil Site 2	10	35.6 \pm 9.2 ^a	9.3 \pm 3.8	13.2 \pm 5.7
	20	22.4 \pm 2.8 ^{a,b}	27.3 \pm 21.7	10.3 \pm 3.4
	30	15.3 \pm 1.3 ^b	11.0 \pm 5.2	6.0 \pm 2.4
	40	18.5 \pm 7.0 ^{a,b}	4.3 \pm 0.4	2.8 \pm 0.3
Topsoil Site 3	10	611 \pm 560	14.1 \pm 2.7	12.2 \pm 2.9
	20	20.8 \pm 1.0	11.2 \pm 2.8	10.3 \pm 6.4
	30	19.7 \pm 1.7	11.3 \pm 2.1	4.2 \pm 0.8
	40	22.6 \pm 6.0	9.9 \pm 5.0	3.2 \pm 0.6
Subsoil Site 1	10	96.4 \pm 41.8 ^a	18.5 \pm 6.3	18.24 \pm 4.6
	20	30.6 \pm 6.9 ^{a,b}	27.5 \pm 14.5	18.64 \pm 8.1
	30	22.5 \pm 9.9 ^b	26.1 \pm 11.0	5.95 \pm 2.1
	40	18.3 \pm 8.1 ^b	11.4 \pm 6.9	12.24 \pm 9.6
Subsoil Site 2	10	120 \pm 20 ^a	25.4 \pm 4.5	26.95 \pm 6.0
	20	22.8 \pm 2.4 ^b	17.3 \pm 2.1	12.20 \pm 5.8
	30	20.9 \pm 1.7 ^b	16.6 \pm 6.8	11.88 \pm 4.3
	40	20.6 \pm 7.4 ^b	29.1 \pm 16.0	12.21 \pm 4.9
Subsoil Site 3	10	60.3 \pm 15.2 ^a	17.0 \pm 6.9	11.73 \pm 6.8
	20	24.1 \pm 3.4 ^b	9.1 \pm 5.0	8.39 \pm 2.7
	30	22.2 \pm 7.1 ^b	53.7 \pm 38.0	5.0 \pm 1.4
	40	18.4 \pm 6.3 ^b	12.8 \pm 5.6	4.1 \pm 1.3

3.4. Microbial Substrate-C Use Efficiency

Microbial C use efficiency (Mic_{eff}) gives an indication of the relative amount ^{14}C immobilized by the microbial community after the addition of DOC or DON substrates (the immobilization-to-mineralization ratio). A comparison of Mic_{eff} between the three sites shows some significant differences ($p \leq 0.05$) (Figure 5) and temperature tended to decrease Mic_{eff} , particularly between 20 °C and 30 °C in all soil types ($p \leq 0.05$).

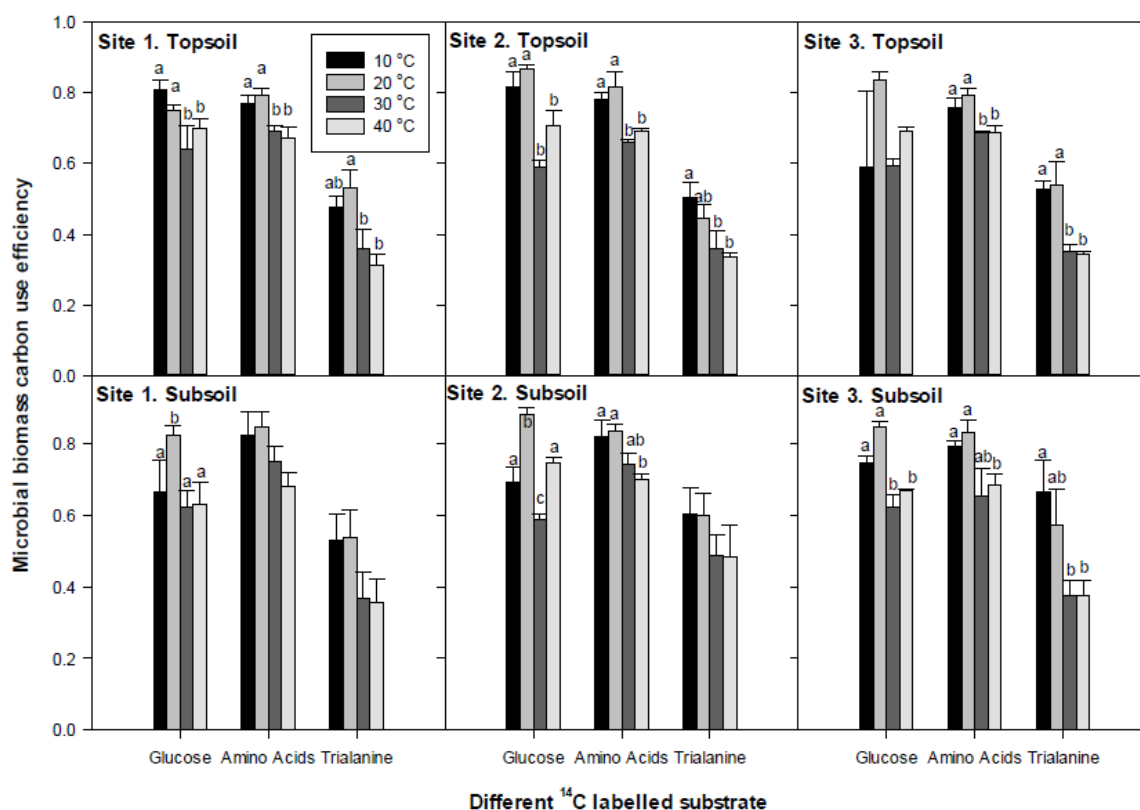


Figure 5. Impact of temperature on microbial carbon-use efficiency for three different C substrates in three arid agricultural oasis sites. Values represent means \pm SEM ($n = 3$). Different letters identify significant differences between temperatures at the $p \leq 0.05$ level. The legend is the same for all panels.

3.5. Temperature Dependency of ^{14}C Respiration Rate

A square root transformation of ^{14}C respiration rate and temperature [43,44] was used to estimate the effect of temperature on the immediate rate of $^{14}CO_2$ production from the labelled substrates added to soil sites (Figure 6). In all cases, the square root value increased with increasing temperature ($p \leq 0.05$). The square root transformation produced a linear fit when plotted against respiration rate with R^2 values ranging from 0.92 to 0.99 for all soils. In almost all cases, no effect was observed between soil sites or depths on the square root of ^{14}C respiration rate ($p > 0.05$).

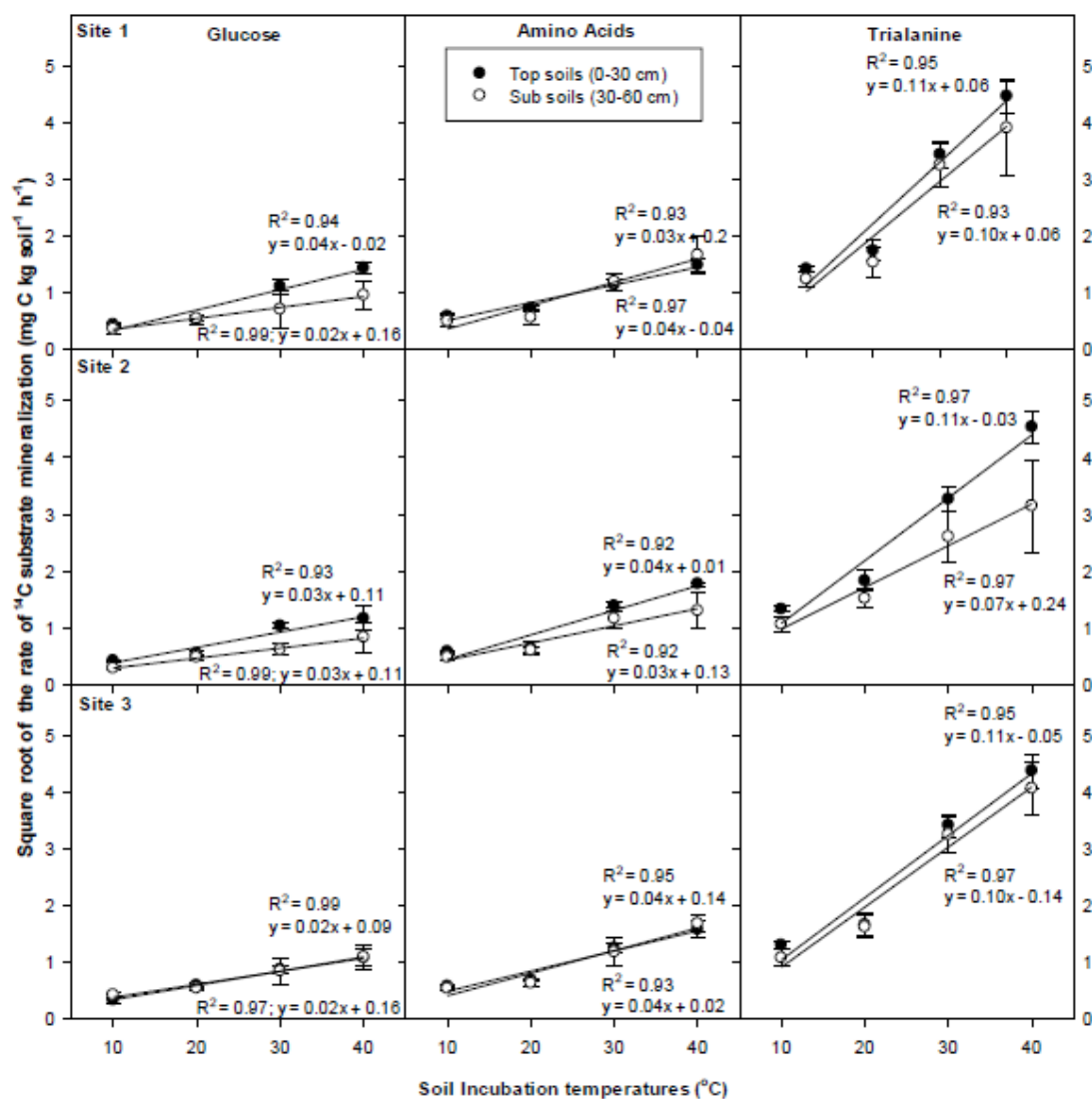


Figure 6. Relationship between soil temperature and the square root of substrate mineralization rate in three different agricultural oasis sites. Points represent means \pm SEM ($n = 3$) while lines represent linear regressions with regression coefficients displayed alongside the lines. The legend is the same for all panels. The substrates (glucose, amino acid and trialanine) are arranged vertically and the sites horizontally within the panels.

4. Discussion

4.1. DON Compounds Mineralization and Half-Life

To our knowledge, the comparison of DON and DOC mineralization responses to temperature in agricultural oasis soils has not previously been reported. To achieve sustainable agriculture in an oasis system and to maintain N fertility, we need to understand the controlling factors that regulate C and N related processes in soil. This study focuses only on the short-term effects of temperature changes on DOC and DON mineralization in three agricultural sites from the Al-Hassa eastern oasis, KSA. We know that the depletion of ^{14}C glucose, ^{14}C amino acids and ^{14}C trialanine in soil can only happen as a result of either abiotic mineralization or microbial uptake [50,51]. Here, we assume that the production of $^{14}\text{CO}_2$ after the addition of radiolabelled substrate was from microbial uptake, since no evolution of $^{14}\text{CO}_2$ was observed from the results of sterile treatments (Figure S1). The range of temperature in this study (10–40 °C) was designed to reflect the actual temperature in soil at the site

and those that might arise in the future. Therefore, we limited our maximum temperature to 40 °C. However, it should be noted that soil surfaces in these arid regions can exceed 65 °C when in direct sunlight [52–54]. These extreme surface temperatures can influence soil processes, soil nutrient and organic matter cycling.

As expected, our results show an increase in substrate partitioning to the fast mineralization pool (a_1) with increasing temperature. This could be due to the microorganisms increasingly using ^{14}C for energy production and cell-maintenance activities (e.g., generation of heat shock proteins, membrane lipid renewal) rather than for growth and storage [41]. This result is consistent with [55], who also showed that the size of C pool a_1 was sensitive to temperature. The results presented in Figures 3 and 4, Tables 4 and 5 generally demonstrate that the rate of $^{14}\text{CO}_2$ evolution from DON > DOC compounds with shorter $t_{\frac{1}{2}}$ for DON substrates, given that the rate of DON turnover is higher than the DOC rate. This could be due to the higher N and C content of DON substrates than DOC substrate for rapidly cycling pool rather than different soil microbial community structure defined by phospholipid fatty acid (PLFA) profiling. Reference [9] reported that the microbial uptake rate of trialanine > dialanine > alanine and could be due to higher N and C contents in trialanine compared to free amino acids. It is also likely that amino acids have higher $^{14}\text{CO}_2$ respiration values than glucose as amino acids are processed by different metabolic pathways inside the cell. After uptake into the cell, amino acids are frequently transaminated or deaminated leading to the production of organic acid skeletons (keto acids), which can be used directly in respiratory pathways [55,56]. This is further supported by continental-scale measures of microbial C-use efficiency in soil microbial communities supplied with sugars and amino acids [57]. In contrast, glucose-derived C is typically preferentially used for producing new cell biomass. This suggestion is also consistent with [55] who showed that amino acids had lower mean residence time through the soil microbial biomass compared to glucose (20 ± 1 days and 40 ± 6 days respectively). This result supports our hypothesis that the mineralization rate of DON is higher than for DOC in arid soils.

Neither site nor depth had a major effect on the amount of $^{14}\text{CO}_2$ evolution or the amount of C partitioned into C pool a_1 . The similarity between agricultural soil sites or depths could be due to their similar soil PLFA microbial communities and to the commonality in metabolic pathways for processing LMW DON or DOC [58]. This could also be due in part to a diverse microbial community having similar affinity transporters for substrate uptake from soil [41]. The lack of influence of soil depth on substrate use in this study differed from [59], who showed that soil depth greatly influenced substrate utilization due to higher microbial activity, biomass, organic matter, C content, and soil pH in topsoil compared to subsoils. We ascribe the lack of effect in this study to there being no significant horizonation within the soil profile and few differences between soil PLFA microbial community, soil pH and initial C content in the different soil layers.

4.2. Microbial Biomass C-Use Efficiency (Mic_{eff})

The results indicate that Mic_{eff} was very similar between the three sites. Overall, increasing temperature tended to decrease Mic_{eff} after the addition of DON and DOC substrates (Figure 5). We hypothesize that temperature directly affects the relative balance of C flow through different metabolic pathways within the community, rather than it being caused by preferential capture by different microbial groups (e.g., bacteria vs. fungi). This result is consistent with others in this field e.g., [23], who show that the Mic_{eff} of glucosamine tends to decrease with increasing temperature due to changing temperature affecting different metabolic pathways of individual C compounds. Differences between Mic_{eff} of peptides and amino acids is potentially interesting. We ascribe the observed response to the differences in the internal partitioning of peptide and amino acid-derived C by the soil microbial biomass. In our experiments we used tri-alanine as a model peptide and a mixture of amino acids (which included alanine). Based on [56] we now know that the Mic_{eff} can be different for individual amino acids. This can be ascribed to: (i) their position within different biosynthetic pathways within the cell and the relative importance of these pathways (i.e., substrate demand); (ii) whether the amino acids are

deaminated or transaminated prior to further use; (iii) whether the products of catabolism lead to the production of keto acids that can be used directly in respiration; and (iv) the relative demand for individual amino acids in protein synthesis. The factors described above help explain our observed differences in relative C partitioning between pools a_1 and a_2 for the amino acids and peptides.

Decreasing Mic_{eff} is often linked to increasing temperatures e.g., [60,61]. It also appears to be a common response found across a range of substrates (mixture of amino acids, amino sugars, sugars, and organic acids) because it is suggested that increased temperature may affect different energy-demanding processes such as increasing C respiration and microbial turnover rate [61]. These results support our hypothesis that the mineralization rate of DON and DOC increases with increasing temperature and that increasing temperature not only speeds up organic matter cycling but also the way the C is subsequently used by the microbial biomass. Typically, mathematical models describing soil organic matter turnover use a Q_{10} factor of 2 to describe how mineralization increases with temperature but they rarely factor in concurrent changes in Mic_{eff} . Based on our results this would indicate that C will be lost at greater rates than predicted from these simple C models.

It should also be noted that Mic_{eff} can be defined in different ways depending on the nature of the study [61]. For example, studies have looked at C partitioning and Mic_{eff} in soil microbial communities supplied with C substrates over short time scales (hours→days), while others have explored Mic_{eff} from food web and ecosystem perspectives (months→years timescale). This makes the standardisation of Mic_{eff} problematic as it is highly dependent on the spatial and temporal scale over which the measurements are made [41,61]. In this study, we are focusing on community-scale efficiency of microbial biomass synthesis [61,62].

4.3. Temperature Dependency of ^{14}C Respiration Rate

Temperature is a regulator of microbial activity in soil and is, therefore, a key control on the speed of soil organic matter turnover. Preserving organic matter in arid soils is central to maintaining soil quality as it is responsible for many beneficial aspects of soil functioning (e.g., increasing aeration, water infiltration, nutrient cycling/retention, providing a habitat for microorganisms, etc.). Factors that lead to the accelerated loss of organic matter need to be better understood so that they can be managed either by eliminating or reducing them or putting in place mitigation strategies to minimise them (e.g., replenishing organic matter reserves). In addition, the loss of organic matter will lead to increased emissions of CO_2 and is likely to lead to enhanced N mineralization which, depending upon the hydrological regime, may lead to excess nitrate leaching. While this may lead to pollution of groundwater and drinking water and indirect N_2O emissions, it also represents an economic loss to farmers.

As expected, our results showed an increase in soil respiration rate with increasing temperature (Figure 6). We suggest that this could be due to microbial communities favouring high temperature for uptake, turnover and metabolism of the added substrate. Reference [63] reported an increase in microbial respiration with increasing temperatures from 5 °C to 25 °C due to the microbial communities favouring catabolic processes of substrate at higher temperature. This could be due to microorganisms using ^{14}C in respiration for maintenance costs at high temperature rather than for growth and storage [54]. This result supports our hypothesis that the mineralization rate of DON and DOC increases with increasing temperature.

5. Conclusions

As expected, soil temperature increased mineralization rate in the three arid soils examined here. For each low molecular-weight substrate, a double exponential decay model conformed well to the experimental mineralization data. This allowed the microbial partitioning of C into catabolic and anabolic processes to be determined for each substrate and soil. Using this approach, we showed significant increases in the amount of substrate-C allocated to microbial catabolic processes with increasing soil temperature. This results in an overall reduction in C-use efficiency within the soil

microbial community. In addition, this study showed an increase in soil respiration rate with increasing temperature. We ascribe this to microorganisms using ^{14}C in respiration for maintenance costs at high temperature rather than for growth and storage. This result supports our hypothesis that the mineralization rate of DON and DOC increases with increasing temperature. The results from our study also showed the rate of $^{14}\text{CO}_2$ evolution from DON > DOC compounds with shorter $t_{\frac{1}{2}}$ for DON substrates, thus proving our second hypothesis that the mineralization rate of DON is higher than for DOC in arid soils. Additional studies are needed to investigate the effect of using alternative sources of irrigation water on soil function, particularly the response of various moisture regimes on soil chemical characteristics and rates of C and N cycling.

Supplementary Materials: The following are available online at <http://www.mdpi.com/2571-8789/2/2/28/s1>.

Author Contributions: All authors were involved in the initial conceptualization (A.A.A., D.J., P.R.), training for the methodology, software and validation was provided by P.R. and D.J., the work was completed by A.A.A.; formal analysis was completed by A.A.A. with guidance from P.R. and D.J.; investigation of the results was conducted by all authors, data is curated by A.A.A.; the original draft was written and prepared by A.A.A. with input from P.R. and D.J.; writing, review and editing was conducted by all authors; visualizations by A.A.A.; supervision by P.R. and D.J., project administration by P.R. and funding was acquired by A.A.A. from the Royal Embassy of Saudi Arabia—Cultural Bureau in London and Imam Abdulrahman Bin Faisal University.

Acknowledgments: This research was supported by the Royal Embassy of Saudi Arabia—Cultural Bureau in London and Imam Abdulrahman Bin Faisal University. We also thank HIDA for allowing their field experiments to be sampled and for their help in sample collection. We would like to thank Agriculture and Veterinary Research Station and Training, King Faisal University, Al-Hassa, KSA, for providing the temperature data.

Conflicts of Interest: The authors declare no conflicts of interest.

References

1. Al-Rawahi, M.N.; Brinkmann, K.; Schlecht, E.; Buerkert, A. Effects of changing water availability on land use in irrigated mountain oases of Al Jabal Al Akhdar, northern Oman. *DIE ERDE J. Geogr. Soc. Berl.* **2014**, *145*, 197–211. [[CrossRef](#)]
2. Asano, T.; Levine, A.D. Wastewater reclamation, recycling and reuse: Past, present, and future. *Water Sci. Technol.* **1996**, *33*, 1–14.
3. Pedrero, F.; Kalavrouziotis, I.; Alarcón, J.J.; Koukoulakis, P.; Asano, T. Use of treated municipal wastewater in irrigated agriculture—Review of some practices in Spain and Greece. *Agric. Water Manag.* **2010**, *97*, 1233–1241. [[CrossRef](#)]
4. Hussain, G.; Al-Saati, A.J. Wastewater quality and its reuse in agriculture in Saudi Arabia. *Desalination* **1999**, *123*, 241–251. [[CrossRef](#)]
5. Al-Kuwaiti, K.A. *Efforts Drainage and Irrigation Authority and its Plans to Provide Irrigation Water from Different Sources (in Arabic)*; Ministry of Agriculture, Al-Hassa Irrigation and Drainage Authority: Al-Hassa, Saudi Arabia, 2010.
6. Aldakheel, Y.Y. Assessing NDVI Spatial Pattern as Related to Irrigation and Soil Salinity Management in Al-Hassa Oasis, Saudi Arabia. *J. Indian Soc. Remote Sens.* **2011**, *39*, 171–180. [[CrossRef](#)]
7. Buerkert, A.; Nagieb, M.; Siebert, S.; Khan, I.; Al-Maskri, A. Nutrient cycling and field-based partial nutrient balances in two mountain oases of Oman. *Field Crops Res.* **2005**, *94*, 149–164. [[CrossRef](#)]
8. Yang, R.; Su, Y.; Yang, Q. Crop Yields and Soil Nutrients in Response to Long-Term Fertilization in a Desert Oasis. *Agron. J.* **2015**, *107*, 83–92. [[CrossRef](#)]
9. Farrell, M.; Hill, P.W.; Farrar, J.; DeLuca, T.H.; Roberts, P.; Kielland, K.; Dahlgren, R.; Murphy, D.V.; Hobbs, P.J.; Bardgett, R.D.; et al. Oligopeptides Represent a Preferred Source of Organic N Uptake: A Global Phenomenon? *Ecosystems* **2013**, *16*, 133–145. [[CrossRef](#)]
10. Hill, P.W.; Farrar, J.; Roberts, P.; Farrell, M.; Grant, H.; Newsham, K.K.; Hopkins, D.W.; Bardgett, R.D.; Jones, D.L. Vascular plant success in a warming Antarctic may be due to efficient nitrogen acquisition. *Nat. Clim. Chang.* **2011**, *1*, 50–53. [[CrossRef](#)]
11. Hill, P.W.; Marsden, K.A.; Jones, D.L. How significant to plant N nutrition is the direct consumption of soil microbes by roots? *New Phytol.* **2013**, *199*, 948–955. [[CrossRef](#)] [[PubMed](#)]

12. Jones, D.L.; Farrar, J.F.; Macdonald, A.J.; Kemmitt, S.J.; Murphy, D.V. Dissolved Organic Nitrogen and Mechanisms of Its Uptake by Plants in Agricultural Systems. In *Quantifying and Understanding Plant Nitrogen Uptake for Systems Modeling*; Liwang, M., Ahuja, L.R., Bruulsema, T., Eds.; CRC Press Taylor and Francis Group: Boca Raton, FL, USA, 2008; pp. 95–126.
13. Javid, M.; Bahramifar, N.; Younesi, H.; Taghavi, S.M.; Givchchi, R. Dry deposition, seasonal variation and source interpretation of ionic species at Abali, Firouzkouh and Varamin, Tehran Province, Iran. *Atmos. Res.* **2015**, *157*, 74–90. [[CrossRef](#)]
14. Li, C.; Li, Y.; Tang, L. The effects of long-term fertilization on the accumulation of organic carbon in the deep soil profile of an oasis farmland. *Plant Soil* **2013**, *369*, 645–656. [[CrossRef](#)]
15. Jones, D.L.; Nguyen, C.; Finlay, R.D. Carbon flow in the rhizosphere: Carbon trading at the soil-root interface. *Plant Soil* **2009**, *321*, 5–33. [[CrossRef](#)]
16. Ferguson, S.D.; Nowak, R.S. Transitory effects of elevated atmospheric CO₂ on fine root dynamics in an arid ecosystem do not increase long-term soil carbon input from fine root litter. *New Phytol.* **2011**, *190*, 953–967. [[CrossRef](#)] [[PubMed](#)]
17. Sivakumar, M.V.K.; Ruane, A.C.; Camacho, J. Climate Change in the West Asia and North Africa Region. In *Climate Change and Food Security in West Asia and North Africa*; Springer: Dordrecht, The Netherlands, 2013; pp. 3–26.
18. Chowdhury, S.; Al-Zahrani, M. Implications of Climate Change on Water Resources in Saudi Arabia. *Arab. J. Sci. Eng.* **2013**, *38*, 1959–1971. [[CrossRef](#)]
19. Hijioka, Y.; Lin, E.; Pereira, J.J.; Corlett, R.T.; Cui, X.; Insarov, G.E.; Lasco, R.D.; Lindgren, E.; Surjan, A. Asia. In *Climate Change 2014: Impacts, Adaptation, and Vulnerability. Part B: Regional Aspects. Contribution of Working Group II to the Fifth Assessment Report of the Intergovernmental Panel on Climate Change*; Field, C.B., V.R. Barros, D.J., Dokken, K.J., Mach, M.D., Mastrandrea, T.E., Bilir, M., Chatterjee, K.L., Ebi, Y.O., Estrada, R.C., Genova, B., et al., Eds.; Cambridge University Press: Cambridge, UK; New York, NY, USA, 2014.
20. Christou, M.; Avramides, E.J.; Jones, D.L. Dissolved organic nitrogen dynamics in a Mediterranean vineyard soil. *Soil Biol. Biochem.* **2006**, *38*, 2265–2277. [[CrossRef](#)]
21. Ge, T.D.; Huang, D.F.; Roberts, P.; Jones, D.L.; Song, S.W. Dynamics of Nitrogen Speciation in Horticultural Soils in Suburbs of Shanghai, China. *Pedosphere* **2010**, *20*, 261–272. [[CrossRef](#)]
22. Boddy, E.; Hill, P.W.; Farrar, J.; Jones, D.L. Fast turnover of low molecular weight components of the dissolved organic carbon pool of temperate grassland field soils. *Soil Biol. Biochem.* **2007**, *39*, 827–835. [[CrossRef](#)]
23. Roberts, P.; Jones, D.L. Microbial and plant uptake of free amino sugars in grassland soils. *Soil Biol. Biochem.* **2012**, *49*, 139–149. [[CrossRef](#)]
24. Li, J.; Li, Z.; Wang, F.; Zou, B.; Chen, Y.; Zhao, J.; Mo, Q.; Li, Y.; Li, X.; Xia, H. Effects of nitrogen and phosphorus addition on soil microbial community in a secondary tropical forest of China. *Biol. Fertil. Soils* **2014**, *51*, 207–215. [[CrossRef](#)]
25. Alkolibi, F. Possible effects of global warming on agriculture and water resources in Saudi Arabia: Impacts and responses. *Clim. Chang.* **2002**, *54*, 225–245. [[CrossRef](#)]
26. Al-Fredan, M.A. Nitrogen Fixing Legumes in the Plant Communities. *Am. J. Environ. Sci.* **2011**, *7*, 166–172. [[CrossRef](#)]
27. Bashour, I.; Sayegh, A. *Methods of Analysis for Soils of Arid and Semi-Arid Regions*; Food and Agriculture Organization of the United Nations: Rome, Italy, 2007; ISBN 978-95-5-105661-5.
28. U.S. Environmental Protection Agency (EPA). Method 3051A: Microwave assisted acid digestion of sediments, sludges, soils, and oils. In *Test Methods for Evaluating Solid Waste, Physical/Chemical Methods*; EPA Publication SW-846 (3rd Edition—Final Update IV); 2007 ISBN Physical/Chemical Methods, SW-846; U.S. Environmental Protection Agency (EPA): Washington, DC, USA, 2007.
29. Burden, A.; Garbutt, R.A.; Evans, C.D.; Jones, D.L.; Cooper, D.M. Carbon sequestration and biogeochemical cycling in a saltmarsh subject to coastal managed realignment. *Estuar. Coast. Shelf Sci.* **2013**, *120*, 12–20. [[CrossRef](#)]
30. Murphy, J.; Riley, J.P. A Modified single solution method for the determination of phosphate in natural waters. *Anal. Chim. Acta* **1962**, *27*, 31–36. [[CrossRef](#)]
31. Swain, T.; Hillis, W.E. The phenolic constituents of *Prunus domestica*. I.—The quantitative analysis of phenolic constituents. *J. Sci. Food Agric.* **1959**, *10*, 63–68. [[CrossRef](#)]

32. Miranda, K.M.; Espey, M.G.; Wink, D.A. A Rapid, Simple Spectrophotometric Method for Simultaneous Detection of Nitrate and Nitrite. *Nitric Oxide Biol. Chem.* **2001**, *5*, 62–71. [[CrossRef](#)] [[PubMed](#)]
33. Mulvaney, R.L. Nitrogen—Inorganic Forms. In *Methods of Soil Analysis: Part 3: Chemical Methods*; Sparks, D.L., Ed.; Soil Science Society of America, Inc., American Society of Agronomy, Inc.: Madison, WI, USA, 1996; pp. 1123–1184.
34. Roberts, P.; Jones, D.L. Critical evaluation of methods for determining total protein in soil solution. *Soil Biol. Biochem.* **2008**, *40*, 1485–1495. [[CrossRef](#)]
35. Jones, D.L.; Owen, A.G.; Farrar, J.F. Simple method to enable the high resolution determination of total free amino acids in soil solutions and soil extracts. *Soil Biol. Biochem.* **2002**, *34*, 1893–1902. [[CrossRef](#)]
36. Buyer, J.S.; Sasser, M. High throughput phospholipid fatty acid analysis of soils. *Appl. Soil Ecol.* **2012**, *61*, 127–130. [[CrossRef](#)]
37. Findlay, R.H. Determination of microbial community structure using phospholipid fatty acid profiles. In *Molecular Microbial Ecology Manual*; Kowalchuk, G.A., Bruijn, F.J.D., Head, I.M., Akkermans, A.D.L., Elsas, J.D.V., Eds.; Kluwer Academic Publishers: Dordrecht, The Netherlands, 2004; pp. 983–1004.
38. Frostegård, Å.; Bååth, E.; Tunlio, A. Shifts in the structure of soil microbial communities in limed forests as revealed by phospholipid fatty acid analysis. *Soil Biol. Biochem.* **1993**, *25*, 723–730. [[CrossRef](#)]
39. Fernandes, M.F.; Saxena, J.; Dick, R.P. Comparison of Whole-Cell Fatty Acid (MIDI) or Phospholipid Fatty Acid (PLFA) Extractants as Biomarkers to Profile Soil Microbial Communities. *Microb. Ecol.* **2013**, *66*, 145–157. [[CrossRef](#)] [[PubMed](#)]
40. Farrell, M.; Hill, W.; Farrar, J.; Wanniarachchi, D.; Bardgett, D.; Jones, D.L. Rapid peptide metabolism: A major component of soil nitrogen cycling? *Glob. Biogeochem. Cycles* **2011**, *25*, 11. [[CrossRef](#)]
41. Glanville, H.C.; Hill, P.W.; Schnepf, A.; Oburger, E.; Jones, D.L. Combined use of empirical data and mathematical modelling to better estimate the microbial turnover of isotopically labelled carbon substrates in soil. *Soil Biol. Biochem.* **2016**, *94*, 154–168. [[CrossRef](#)]
42. Jones, D.L.; Olivera-Ardid, S.; Klumpp, E.; Knief, C.; Hill, P.W.; Lehdorff, E.; Bol, M. Moisture activation and carbon use efficiency of soil microbial communities along an aridity gradient in the Atacama Desert. *Soil Biol. Biochem.* **2018**, *117*, 68–71. [[CrossRef](#)]
43. Birgander, J.; Reischke, S.; Jones, D.L.; Rousk, J. Temperature adaptation of bacterial growth and ¹⁴C-glucose mineralisation in a laboratory study. *Soil Biol. Biochem.* **2013**, *65*, 294–303. [[CrossRef](#)]
44. Rousk, J.; Frey, S.D.; Bååth, E. Temperature adaptation of bacterial communities in experimentally warmed forest soils. *Glob. Chang. Biol.* **2012**, *18*, 3252–3258. [[CrossRef](#)] [[PubMed](#)]
45. Al-Jasser, A.O. Saudi wastewater reuse standards for agricultural irrigation: Riyadh treatment plants effluent compliance. *J. King Saud Univ. Eng. Sci.* **2011**, *23*, 1–8. [[CrossRef](#)]
46. Ayers, R.S.; Westcot, D.W. *Water Quality for Agriculture*; Food and Agriculture Organization of the United Nations: Rome, Italy, 1985; Volume 29, ISBN 92-5-102263-1.
47. Certini, G.; Scalenghe, R. *Soils: Basic Concepts and Future Challenges*; Cambridge University Press: Cambridge, UK, 2006.
48. Boulding, J.R. *Description and Sampling of Contaminated Soils: A Field Guide*, 2nd ed.; CRC Press: Boca Raton, FL, USA, 1994.
49. Food and Agriculture Organization of the United Nations (FAO). *Near East Fertilizer—Use Manual*; Food and Agriculture Organization of the United Nations: Rome, Italy, 2006.
50. Hill, P.W.; Farrar, J.F.; Jones, D.L. Decoupling of microbial glucose uptake and mineralization in soil. *Soil Biol. Biochem.* **2008**, *40*, 616–624. [[CrossRef](#)]
51. Jan, M.T.; Roberts, P.; Tonheim, S.K.; Jones, D.L. Protein breakdown represents a major bottleneck in nitrogen cycling in grassland soils. *Soil Biol. Biochem.* **2009**, *41*, 2272–2282. [[CrossRef](#)]
52. Nobel, P.S. Extreme temperatures and thermal tolerances for seedlings of desert succulents. *Oecologia* **1984**, *62*, 310–317. [[CrossRef](#)] [[PubMed](#)]
53. Garratt, J.R. Extreme Maximum Land Surface Temperatures. *J. Appl. Meteorol.* **1992**, *31*, 1096–1105. [[CrossRef](#)]
54. Williams, J.B.; Tieleman, B.I.; Shobrak, M. Lizard Burrows Provide Thermal Refugia for Larks in the Arabian Desert. *Condor* **1999**, *101*, 714–717. [[CrossRef](#)]
55. Boddy, E.; Roberts, P.; Hill, P.W.; Farrar, J.; Jones, D.L. Turnover of low molecular weight dissolved organic C (DOC) and microbial C exhibit different temperature sensitivities in Arctic tundra soils. *Soil Biol. Biochem.* **2008**, *40*, 1557–1566. [[CrossRef](#)]

56. Jones, D.L.; Kemmitt, S.J.; Wright, D.; Cuttle, S.P.; Bol, R.; Edwards, A.C. Rapid intrinsic rates of amino acid biodegradation in soils are unaffected by agricultural management strategy. *Soil Biol. Biochem.* **2005**, *37*, 1267–1275. [[CrossRef](#)]
57. Jones, D.L.; Hill, P.W.; Smith, A.R.; Farrell, M.; Ge, T.; Banning, N.C.; Murphy, D.V. Role of substrate supply on microbial carbon use efficiency and its role in interpreting soil microbial community-level physiological profiles (CLPP). *Soil Biol. Biochem.* **2018**, in press.
58. Hill, P.W.; Farrell, M.; Roberts, P.; Farrar, J.; Grant, H.; Newsham, K.K.; Hopkins, D.W.; Bardgett, R.D.; Jones, D.L. Soil-and enantiomer-specific metabolism of amino acids and their peptides by Antarctic soil microorganisms. *Soil Biol. Biochem.* **2011**, *43*, 2410–2416. [[CrossRef](#)]
59. Rukshana, F.; Butterly, C.R.; Xu, J.M.; Baldock, J.A.; Tang, C. Soil organic carbon contributes to alkalinity priming induced by added organic substrates. *Soil Biol. Biochem.* **2013**, *65*, 217–226. [[CrossRef](#)]
60. Manzoni, S.; Taylor, P.; Richter, A.; Porporato, A.; Ågren, G.I. Environmental and stoichiometric controls on microbial carbon-use efficiency in soils. *New Phytol.* **2012**, *196*, 79–91. [[CrossRef](#)] [[PubMed](#)]
61. Schindlbacher, A.; Schneckler, J.; Takriti, M.; Borke, W.; Wanek, W. Microbial physiology and soil CO₂ efflux after 9 years of soil warming in a temperate forest—No indications for thermal adaptations. *Glob. Chang. Biol.* **2015**, *21*, 4265–4277. [[CrossRef](#)] [[PubMed](#)]
62. Geyer, K.M.; Snowman, E.K.; Grandy, A.S.; Frey, S.D. Microbial carbon use efficiency: Accounting for population, community, and ecosystem-scale controls over the fate of metabolized organic matter. *Biogeochemistry* **2016**, *127*, 173–188. [[CrossRef](#)]
63. Agehara, S.; Warncke, D.D. Soil Moisture and Temperature Effects on Nitrogen Release from Organic Nitrogen Sources. *Soil Sci. Soc. Am. J.* **2005**, *69*, 1844. [[CrossRef](#)]



© 2018 by the authors. Licensee MDPI, Basel, Switzerland. This article is an open access article distributed under the terms and conditions of the Creative Commons Attribution (CC BY) license (<http://creativecommons.org/licenses/by/4.0/>).